

# Deposition time and annealing effects on morphological and optical properties of ZnS thin films prepared by Chemical Bath Deposition

N. Chabou<sup>1</sup>, B. Birouk<sup>2</sup>, M.S. Aida<sup>3</sup>, J.P. Raskin<sup>4</sup>

<sup>1,2</sup>Renewable Energies Laboratory (LER)/ Jijel University, Algeria

<sup>3</sup>Thin Films and Interfaces Laboratory, Constantine University, Algeria

<sup>4</sup>ICTEAM/ Université catholique de Louvain (UCL), Louvain-La-Neuve, Belgium

<sup>1</sup>[chabounawel@yahoo.fr](mailto:chabounawel@yahoo.fr); <sup>2</sup>[bbirouk@gmx.com](mailto:bbirouk@gmx.com); <sup>4</sup>[jean-pierre.raskin@uclouvain.be](mailto:jean-pierre.raskin@uclouvain.be)

## Abstract

The nanocrystalline Zinc Sulfide (ZnS) thin films are prepared on glass substrates by chemical bath deposition (CBD) method using aqueous solutions of zinc chloride, thiourea ammonium hydroxide along with non-toxic complexing agent tri-sodium citrate in alkaline medium at 80 °C. The deposition time and annealing effects on the optical and morphological properties are studied. The morphological, compositional, and optical properties of films are investigated by scanning electron microscopy (SEM), X-ray energy dispersive spectroscopy (EDAX) and UV-Visible spectroscopy. SEM micrographs exhibit uniform surface coverage. UV-visible (300–800 nm) spectrophotometric measurements show transparency of the films (transmittance ranging from 69 to 81%), with a direct allowed energy band gap in the range of 3.78 – 4.03 eV. After thermal annealing at 500°C for 120 min, the transmittance increases up to 87%.

**Keywords:** CBD, ZnS, Complexing Agent, stirring Annealing.

## 1- Introduction

The development of materials in the form of thin layers is of major interest in a wide range of applications. These thin layers have in particular different physicochemical properties from those of bulk materials. Metals chalcogenides are semiconductors which have attracted a lot of attention these last years because of their remarkable physical properties in optoelectronic applications, as well as in solar cells fabrication as a buffer layer. Nowadays, the most used among these materials is the zinc sulfide. ZnS has a large direct band gap (3.65–3.7 eV), high refractive index (2.25–2.35), and great exciton binding energy of 40 meV with n-type electrical conductivity. It is considered as one of the most suitable candidates for field emitters [1], and field effect transistors (FETs) [2]; an ideal object for fabrication of high-performance sensors and of great importance for applications in infrared windows [3] and lasers [4]. ZnS thin films have been found valuable as buffer layer in replacement of the harmful CdS in CIGS thin film solar cells.

Different techniques can be used to deposit such material in thin film which originate from purely physical or purely chemical processes such as close-spaced vacuum sublimation technique (CSV) [5], pulse plated [6], thermal evaporation [7], successive ionic layer adsorption and reaction (SILAR) [8], RF magnetron sputtering [9], chemical vapor deposition (CVD) [10], electrodeposition [11], spray pyrolysis [12], and flash evaporation technique [13]. The physical properties of the material are strongly dependent on the methods of preparation. We chose the method called CBD as the technique is relatively simple, economical and cost effective, can be carried out at lower temperature and pressure, it is easily coated over large surfaces, also this method allows to deposit optically smooth, uniform and homogeneous layers. Chemical bath deposition was used to deposit ZnS semiconductors [14]. The quality of the deposited film depends on the bath parameters like temperature, time of deposition, concentration of the reactants and the pH of the chemical bath. . A recently, thin film solar cells based on chemical bath deposition ZnS(O,OH) buffer layer have achieved an efficiency of 18.6% [15].

In this work ZnS thin films were deposited by the chemical bath deposition technique. The thin films were prepared from zinc chloride  $ZnCl_2$ , Thiourea ( $SC(NH_2)_2$ ) and ammonium hydroxide ( $NH_4OH$ ). We then study the effect of the deposition time and annealing on the growth and properties of CBD ZnS films. The typical feature of this study of deposition is the use of trisodium citrate ( $C_6H_5Na_3O_7$ ) as second complexing agent to deposit ZnS thin films in aqueous alkaline baths without stirring the reaction bath. The  $Na_3$ -citrate is the most complexing agent among the non-toxic complexing agents. These films were characterized for their structural, morphological and optical properties by using X-ray diffraction, scanning electron microscopy and optical absorption studies.

## 2-Experimental

### 2-1 Reaction mechanism

The CBD process enables the deposition of thin films on substrates submerged in solutions containing chalcogenide source, metal ion, and chelating agent. The latter is used to limit the hydrolysis of the metal ion and impart some stability to the bath. The deposition rate may be controlled by adjusting: the temperature of the bath, the pH, the stirring rate and the relative concentration of the reactants within the solution (chalcogenide source, chelating agent and/or metal ion). Formation of ZnS film will take place when ionic product of  $Zn^{2+}$  and  $S^{2-}$  ions exceeds the solubility product of ZnS. ZnS thin film deposition is based on the slow release of  $Zn^{2+}$  and  $S^{2-}$  ions in the chemical solutions which then condense on the glass substrate.

In aqua solution, zinc chloride ( $ZnCl_2$ ) dissolves and gives  $Zn^{2+}$  ion. Also, in alkaline medium thiourea releases  $S^{2-}$  ions. Ammonia reacts with water and gives  $OH^-$  ions. These  $OH^-$  ions form with  $Zn^{2+}$  complex  $Zn(NH_3)_4^{2+}$ . Therefore, suitable complexing agents should be used to limit the free  $Zn^{2+}$  concentration and decreases the formation of zinc hydroxide and finally zinc oxide.

The various reactions involved in the ZnS growth process can be explained by the following equations:

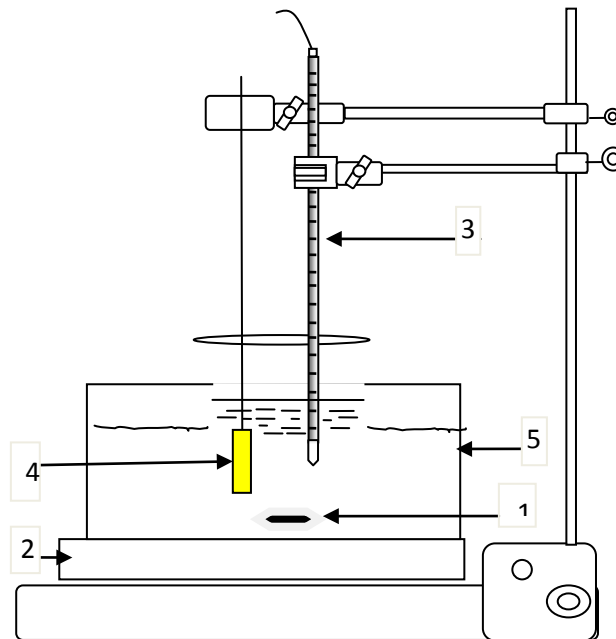


### 2-2 Deposition of ZnS thin films

ZnS thin films are deposited on glass substrates by CBD technique. First of all, the substrate is cleaned in deionized (D.I.) water, then cleaned with methanol and acetone, again rinsed in distilled water and dried in air. The degreased substrate favors nucleation centers for the growth of the films thus giving highly adhesive and uniform films. The ZnS thin films are chemically grown on glass substrates zinc chloride ( $ZnCl_2$ ) as  $Zn^{2+}$  ions source and thiourea  $SC(NH_2)_2$  as  $S^{2-}$  ions source and ammonium hydroxide ( $NH_4OH$ ), trisodium citrate as complexing agents limiting the concentration of  $Zn^{2+}$ , and soluble species of  $Zn^{2+}$  in an aqueous medium.

In the first step, 20 ml of 0.1 M of  $ZnCl_2$  and 40 ml of 0.6 M solution of trisodium citrate ( $C_6H_5Na_3O_7$ ) are mixed and stirred for 30 minutes. Then, 20 ml of 0.8 M solution of thiourea is added slowly to the mixed solution under stirring condition after and in order to obtain the  $pH = 11$ , a sufficient amount of ammonia is added to the solution. Deionized water is added to give the total volume of the solution

100 ml. The agitation is stopped. Thereafter, the glass substrates are immersed vertically inside this beaker. All reagents are of high analytical grade. Fig. 1 shows the experimental setup for chemical bath deposition technique.



1 - Stirrer, 2 - Hot plate, 3 – Thermocouple, 4 - Substrate, and 5 - Reactive aqueous solution.

**Fig. 1:** Experimental setup for chemical bath deposition of thin film.

The deposited film is prepared at water bath temperature  $T_b=80^\circ\text{C}$ , for different durations (30, 60, 90, and 120 min). When the deposit reactions are completed, each sample is removed from the beaker and is cleaned with de-ionized water and dried in air to remove the loosely adhered ZnS particles on the films. The deposit obtained is in the form of a white-wish, uniform, transparent, and well adherent film. Then, the ZnS film prepared at  $80^\circ\text{C}$  for 90 min is annealed at  $500^\circ\text{C}$  during 2 hours after deposition.

The transmittance spectrum of ZnS thin film was recorded by UV-Vis (Shimadzu UV-3101) spectrophotometer in the range 300 to 800 nm. The X-ray diffraction (XRD) patterns of the film were recorded using the PHILIPS PW 3710 diffractometer operating at 40 kV, 20 mA and  $\lambda_{\text{CuK}\alpha}=1.54 \text{ \AA}$ . The surface morphology of the films was measured by scanning electron microscopy (SEM). Infrared spectrum of the film deposited on silicon substrate was recorded using Fourier Transform infrared spectrophotometer and the composition of the film was obtained by energy-dispersive X-ray spectroscopy.

### 3-Results and discussion

#### 3-1 Thin films growth

In order to explain the influence of deposition time on the formation of ZnS films, the films are deposited at various deposition times namely 60, 90, 120 and 150 min. The variation of the film thickness with deposition time is shown in Fig. 2. It seems clear that the ZnS films deposited at longer time (120 and 150 min) produced thicker films compared with shorter deposition period. At the deposition time of 60 min, the thickness of thin film is 201 nm while it steadily increases with time and the ZnS thin film has shown higher thickness of 612 nm at the deposition time of 150 min. This result explains that an increase in deposition duration induced more materials to be deposited on substrates and thicker films to be obtained. These results are in agreement with what is reported in the literature.

In any case, at the beginning of the film deposition, the growth is controlled by the ion-by-ion growth mechanism, and then cluster cluster mechanism eventually becomes dominant with the deposited time. In Figure 2, we have reported also the variation of the deposition rate as a function of deposition time. The ZnS film prepared at 80°C for 150 min shows a maximum film growth rate (about 4.08 nm/min).

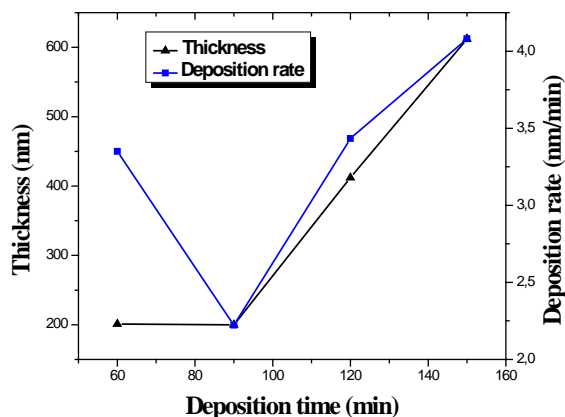


**Fig. 2.** Thickness variation and deposition rate of ZnS thin films at different deposition times.

### 3-2 Structural properties

Figure 3 shows XRD pattern of as-deposited ZnS thin film. This figure does not show any peaks, this is because the layer was formed of very small grains. This result confirms that the film is amorphous. It can be concluded that low deposition temperature (below 100°C) cannot provide the energy required for film growth in a short period of time.

ZnS thin films deposited via the chemical bath are highly disordered, but its microstructure can be transformed by annealing [16].

The XRD patterns of the ZnS film before and after annealing are shown in Fig. 3, (a) and (b). The spectra are obtained by scanning  $2\theta$  in the range of 20°-40° with a grazing angle. After annealing, the diffraction peak originated at  $2\theta = 29.5^\circ$  corresponds to the (008) reflections of the hexagonal phase of ZnS. Göde *et al.* reported that a wurtzite phase takes place at 80°C after annealing [17].

Many works have shown that ZnS film also contains a large amount of ZnOH and ZnO [19]. The formation of ZnO after annealing could be due to film oxidation during annealing or to the thermal decomposition of ZnOH.

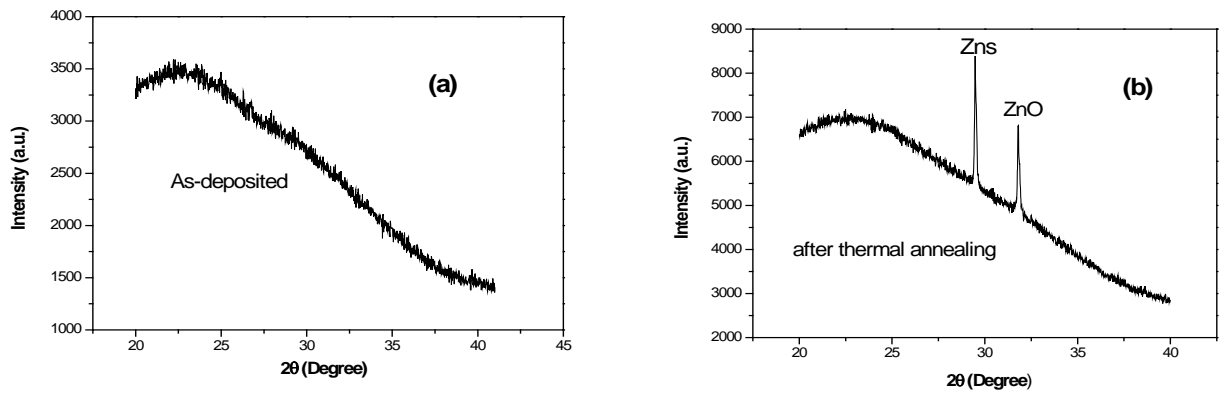
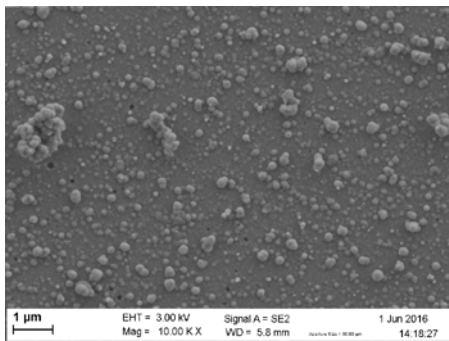


Fig 3. X-ray diffraction patterns of (a) as-deposited and (b) after annealed ZnS thin films deposited at 80°C.

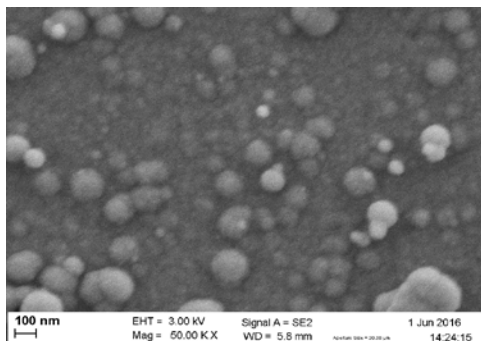
### 3-3 Scanning Electron Microscopy (SEM)

Scanning Electron Microscopy (SEM) is a suitable technique to study the microstructure of thin films. This technique allows to specify the mode of growth via the study of a surface roughness and to determine the effect of the different deposition times on the film morphology.

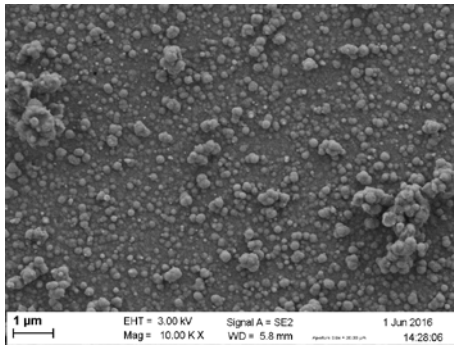
Figure 4 shows the surface morphology of ZnS thin films deposited at temperature 80°C, at different deposition times, observed by SEM. From the micrographs, it is observed that the as-deposited films have uniform morphology with good surface coverage on the substrate (ion-by-ion mechanism) over which freely adherent clusters of grains (cluster-by-cluster mechanism). The ZnS thin films indicate a surface structure consisting of various small particles free of pinholes. When the deposit time increases the particle size increases from around 10 to 20 nm. We can conclude that the homogeneity, grain size and adhesion to the substrate can be increased by the deposition time.



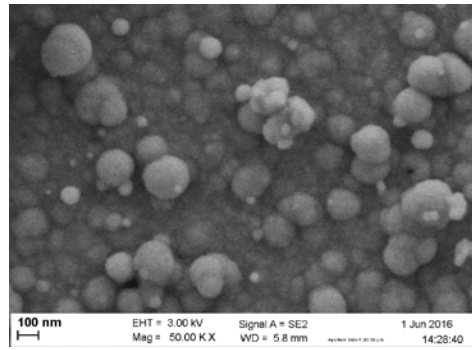
(a)



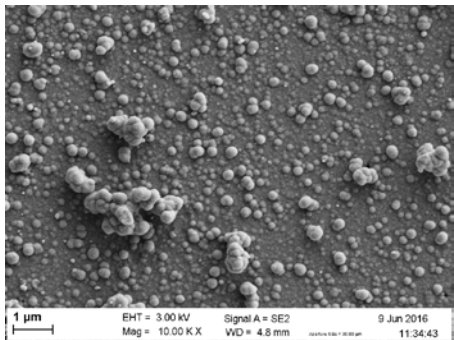
(b)



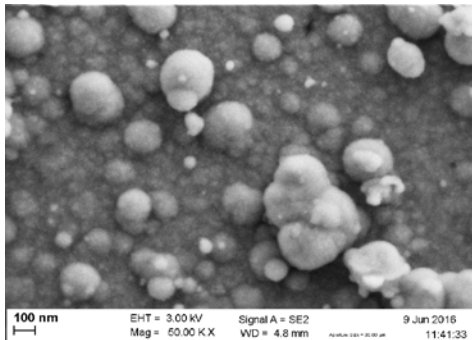
(c)



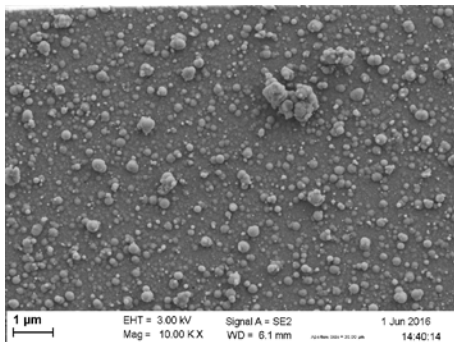
(d)



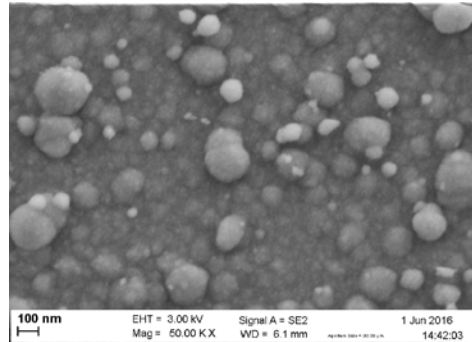
(e)



(f)



(g)



(h)

**Fig. 4 :** SEM images of ZnS thin films deposited at various periods of time:

**(a)** 60 min, **(b)** 90 min, **(c)** 120 min, **(d)** 150 min, **(e-h)** These images are high magnifications of (a–d).

We have estimated by observing the SEM images that the grains size of the films, as a function of deposition time, evolves like it is presented in Table 1.

Table 1: Mean ZnS grains size as a function of deposition time deduced from SEM.

<b>SEM image</b>	<b>Deposition time (min)</b>	<b>Grains size (nm)</b>
4(a)	60	10
4(b)	90	17
4(c)	120	22
4(d)	150	20

Chemical composition of ZnS thin films on glass substrate are analyzed by energy-dispersive X-ray analyzer (EDX) (Figure 5). The EDX analysis confirms the presence of zinc and sulfur in ZnS thin films. We see that the percentage of sulfur is low in the film and it is probably due to the volatility of sulfur.

Excess of Zn may be caused by an amount of Zn(OH)<sub>2</sub> or ZnO originated from the alkaline reaction solution [18]. In the analysis, the presence of the peaks of O, Si, Mg, Cl and Na can be attributed to the amorphous nature of the glass substrate.

Nakada *et al.* [19] suppose that oxygen atoms in the ZnS film deposited by CBD method might be in the compounds of ZnO and Zn(OH)<sub>2</sub>.

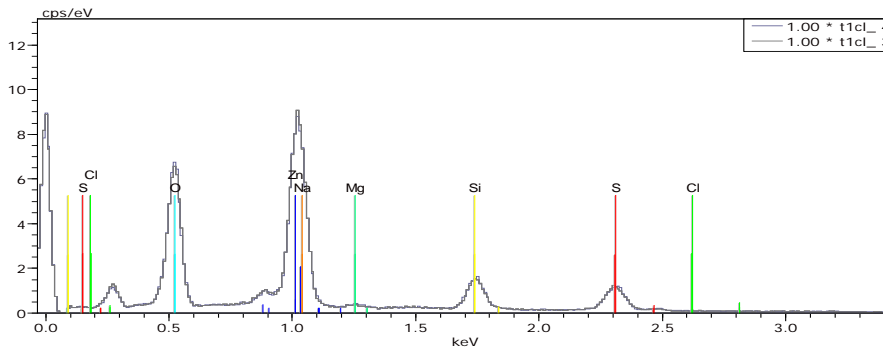


**Fig. 5:** The EDX scanning pattern of the ZnS deposited at 80 °C for 60 min.

### 3-4 Optical properties

The optical properties of ZnS thin films were determined from the variation of the optical transmission with UV-Visible light wavelength  $\lambda$  ranging from 300 to 800 nm.

#### Transmittance:

Figure 6 shows optical transmission spectrum of ZnS thin films for different deposition times, before and after annealing at 500°C during 2 hours.

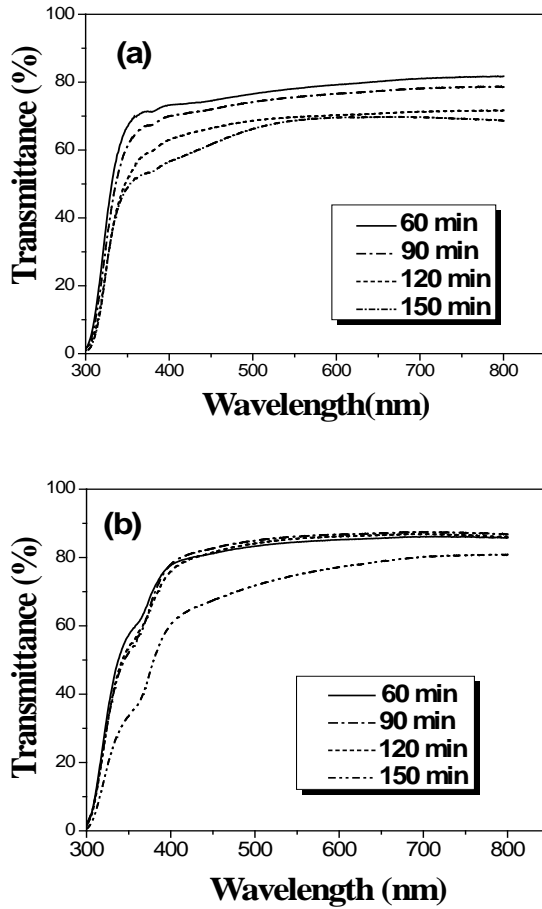


**Fig. 6:** Transmittance spectra of the ZnS films grown on glass substrate with various deposition times. (a) as-deposited, (b) annealed at 500°C for 2 h.

It is clear that the transmittance decreases with the increase of deposition times, before as well as after annealing. This decrease in transmittance can be explained by the evolution of the thickness, in other words increasing the deposition time leads to thicker films. It has been observed that films have a maximum transmittance of 81.7% in the visible region for as deposited films. This high transparency in the visible region indicates that there are not colloid particles formed by homogeneous reaction on the substrate surface. This result is in agreement with SEM micrographs. The average transmittance in the visible range of the film deposited at 90 min is about 87.4 %, which is higher than that deposited at 150 min. Annealing process of the as-deposited films increases the optical transmittance. This increase could be attributed to the rearrangement and decrease of the films defects.

### Absorbance and Reflectance

Fig. 7 and 8 show the spectral variations of the reflectance and absorbance for as-deposited and annealed films. It can be seen that all the samples of ZnS films exhibit high absorbance in UV regions. In the visible region, it weakly absorbs. Also, the values for the annealed film are the lowest compared with the others because the annealed film has a higher transmission values.

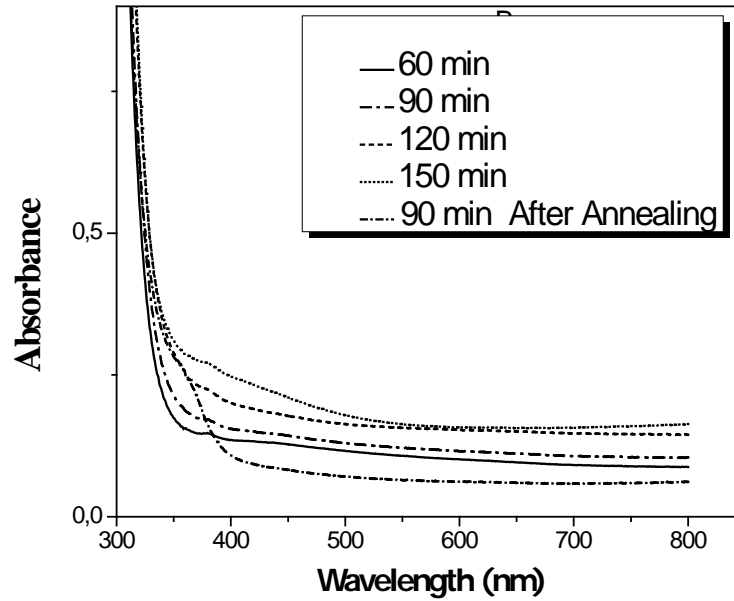


**Fig. 7:** Optical absorbance of nanocrystalline ZnS thin films versus wavelength at different deposition times before and after annealing

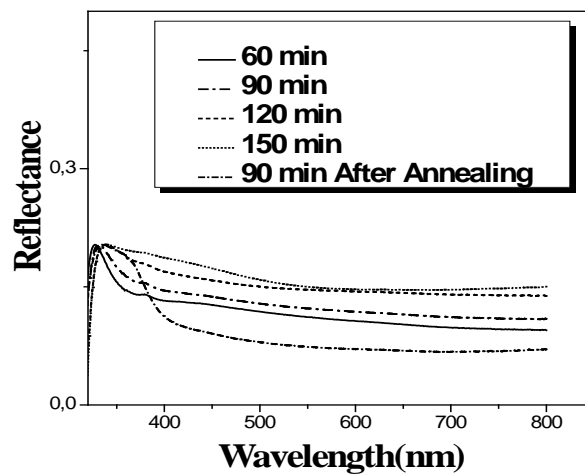


**Fig. 8:** Optical reflectance of nanocrystalline ZnS thin films versus wavelength at different deposition times before and after annealing.

### Absorption coefficient and optical band gap

The  $\alpha$  coefficient for as-deposited and annealed ZnS films are calculated by the following relationship:

$$\alpha = 2.3026 A/t , \quad (5)$$

where A is the absorbance and t is the sample thickness.

In Figure 9, the variation of  $\alpha$  versus wavelength for ZnS nanocrystalline thin layers with deposition time as parameter is reported. One can clearly see that the absorption coefficient of ZnS films increases with the decrease of wavelength.

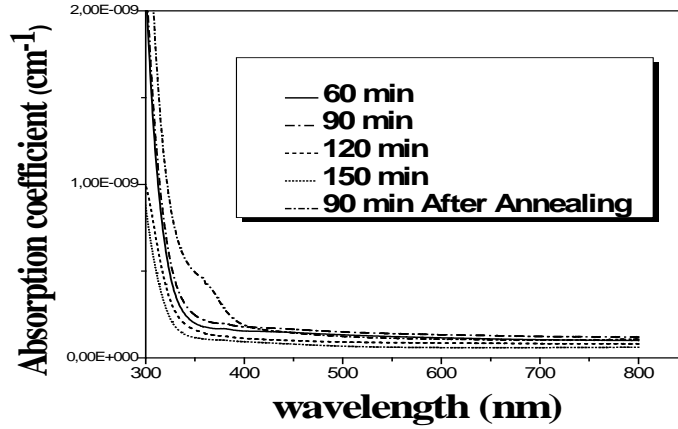


**Fig. 9:** Absorption coefficient of ZnS thin films versus wavelength at different deposition times before and after annealing.

The absorption coefficient values are used to determine the optical energy gap by using the Tauc relationship which is given by the formula:

$$\alpha h\nu = \beta(h\nu - E_g)^n \quad (6)$$

In which,  $h\nu$  is the photon energy,  $E_g$  is the optical band gap of the semiconductor,  $\beta$  is a constant and  $n = 1/2$  for direct band gap semiconductor such as ZnS.

The optical band gap value of the ZnS thin films is estimated by extrapolation of the straight line of the plot of  $(\alpha h\nu)^2$  versus photon energy as it is shown in Figure 10. We found that the  $E_g$  value for the films prepared at different deposition times varies from 3.78 to 4.03 eV, which is in agreement with what is reported by other authors [20]. The band-gap values are higher than the 3.7 eV measured in case of bulk zinc sulfide. This increase may be due to quantum confinement in the small crystals [21]. Also, the increase may be due to the presence of zinc hydroxide produced by the alkaline bath, thereby forming a mixture of zinc sulfur hydroxide Zn(S,OH) [22].

It is clear from Figure 10 that the gap energy values of the films before annealing are greater than that after annealing. The decrease in films band gap width after annealing could be attributed to improvement in the crystal structure and grain sizes change of the films after annealing. Table 1 shows the results of the optical energy gap of ZnS thin films before and after annealing [23].

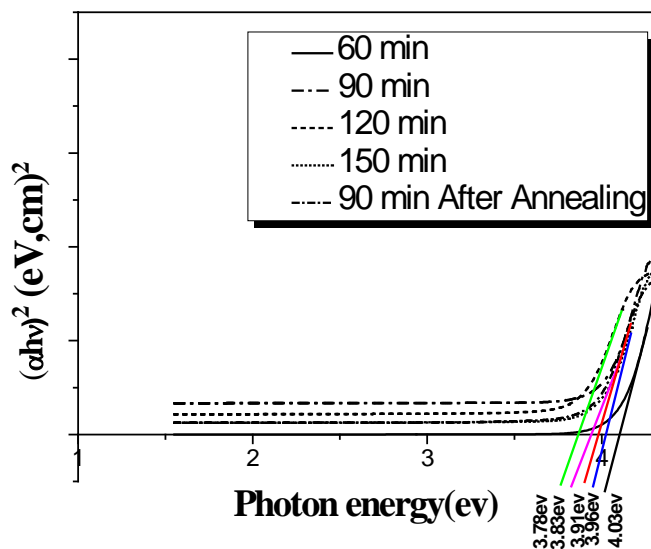


**Fig. 10:**  $(\alpha h\nu)^2$  plots versus photon energy for ZnS thin films deposited at different deposition times, before and after annealing.

**Table 2:** Gap energy values of ZnS thin films, before and after annealing.

Deposition time (min)	Direct band gap energy $E_g$ (eV)	
	Before annealing	After annealing
60	4.03	-
90	3.91	3.83
120	3.78	-
150	3.96	-

The tail width  $E_{00}$  in the gap energy was obtained by plotting  $\ln(\alpha)$  as a function of  $h\nu$ . The inverse of the slope extracted from the linear part gives  $E_{00}$  for deposited ZnS films, as shown in Fig. 11. The  $E_{00}$  value increases with increasing of deposition time until it reaches the value of 120 min after which tail width decreases. This result may be due to the fact that the increase in deposition time implies an increase in films thickness (until  $t=120$  min) and this leads to an increase in film defects and localized states in the gap. As can be seen, the variation of optical gap is opposite to the disorder. This behavior indicates clearly that the optical gap is also controlled by disorder in the film.

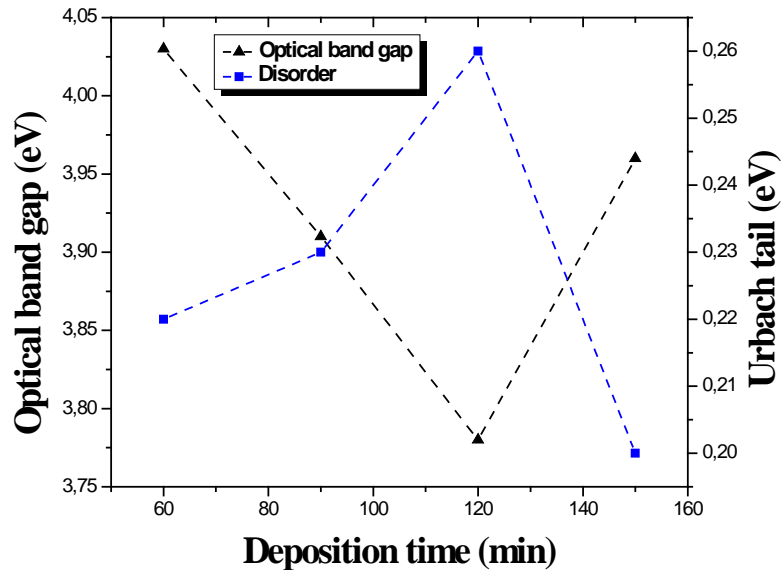


**Fig. 11:** Optical gap and disorder variations of CBD-ZnS thin films as a function of the deposition time.

### Extinction Coefficient (k)

The extinction coefficient (K) is estimated from the following equation:

$$k = \alpha\lambda/4\pi, \quad (7)$$

where  $\lambda$  is the incident radiation wavelength.

Figure 12 shows the evolution of the extinction coefficient as a function of wavelength for different deposition times of ZnS films. The extinction coefficient decreases as the wavelength increases and moreover it increases when the deposition time increases. This decrease in extinction coefficient would be the result of increased surface roughness, as the film thickness increase which respectively, induce the increase of surface optical scattering and extinction coefficient.

Fig. 12 shows also the extinction coefficient of the sample annealed at 500°C for 120 min. From this figure, it is raised that the annealing process leads to the decrease of the extinction coefficient. This might be caused by the fact that the annealing process minimizes the defects or the tails deep (which means decreasing in the film absorbance).

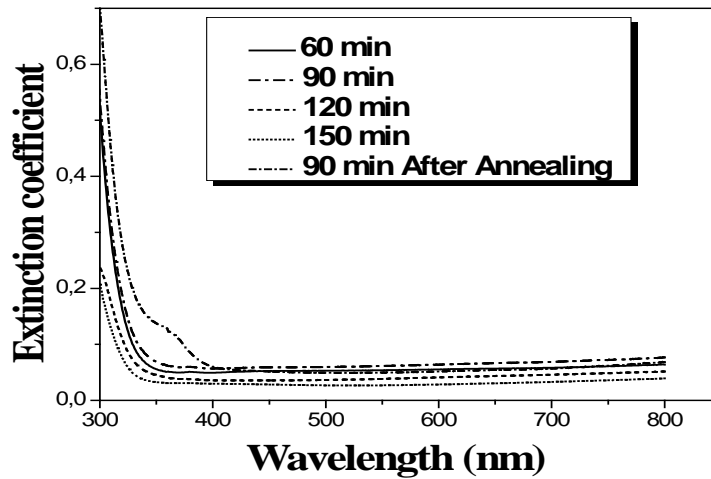


**Fig. 12:** Extinction coefficient of nanocrystalline ZnS thin films versus wavelength, at different deposition times, before and after annealing.

### Refractive Index (n)

The refractive index is determined from transmittance spectra, as function of wavelength, using simple approximated relationship:

$$n = \frac{1+R}{1-R} + \left[ \frac{4R}{(1-R)^2} - k^2 \right]^{1/2}, \quad (8)$$

where R is the reflectance for any intermediate energy photon recorded by spectrophotometer, and k the extinction coefficient.

The refractive index variations on the wavelength range 300-800 nm, for different deposition times, are shown in Figure 13. It results that the refractive index increases when increasing the deposition time in the range spreading from 60 to 150 min. This may be due to the film thickness increase and the formation of non-stoichiometric oxide phases in the ZnS films [24].

The figure also shows the effect of annealing process on the refractive index. It is clear that the annealing process induces a decrease in the refractive index values. After the annealing, the refractive index of the films is lowered by about 10% in the visible range. This decrease is attributed to the fact that ZnS film surface begins to be oxidized when film is annealed at 500°C.

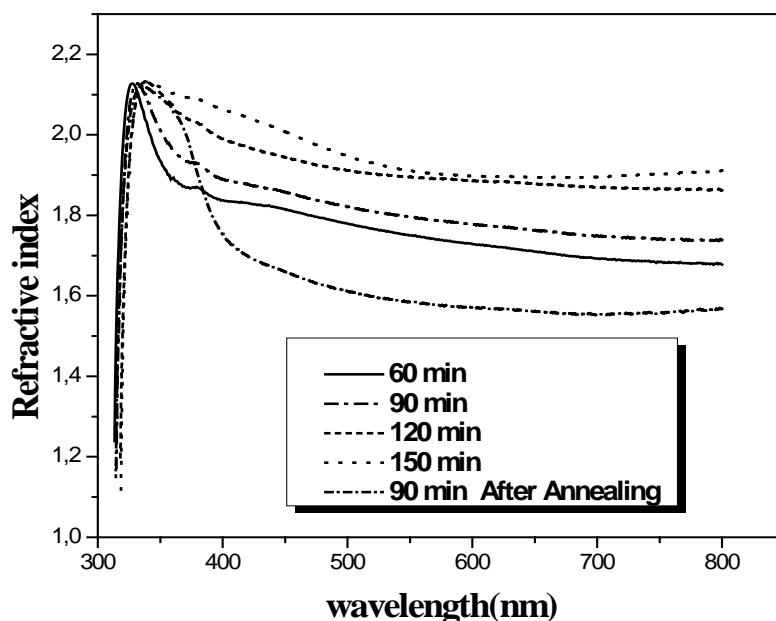


**Fig. 13:** Refractive index of nanocrystalline ZnS thin films versus wavelength at different deposition times, before and after annealing.

Moreover, Fourier Transform Infrared (FTIR) studies were used to verify the presence of ZnS and other impurities present on the surface of the films.

Figure 14 shows the measured FTIR spectra for the films of ZnS deposited at different deposition times on glass and monocrystalline silicon substrates. The absorption band located at  $615\text{ cm}^{-1}$  can be attributed to the formation of ZnS phase [25]. The spectra show a large peak centered at  $3360\text{ cm}^{-1}$  and a small peak at  $1630\text{ cm}^{-1}$ , which are due to stretching and bending modes of H-OH. This might be due to trace amount of adsorbed water present on the film surface. The spectra show a small peak at  $1110\text{ cm}^{-1}$  which is assigned to stretching mode of Zn-OH. The spectra also show a weak band in the region of  $1475\text{ cm}^{-1}$ , which could be due to the bending modes of C-H. Based on this study, we can say, the film contains some amount of  $\text{Zn}(\text{OH})_2$ .

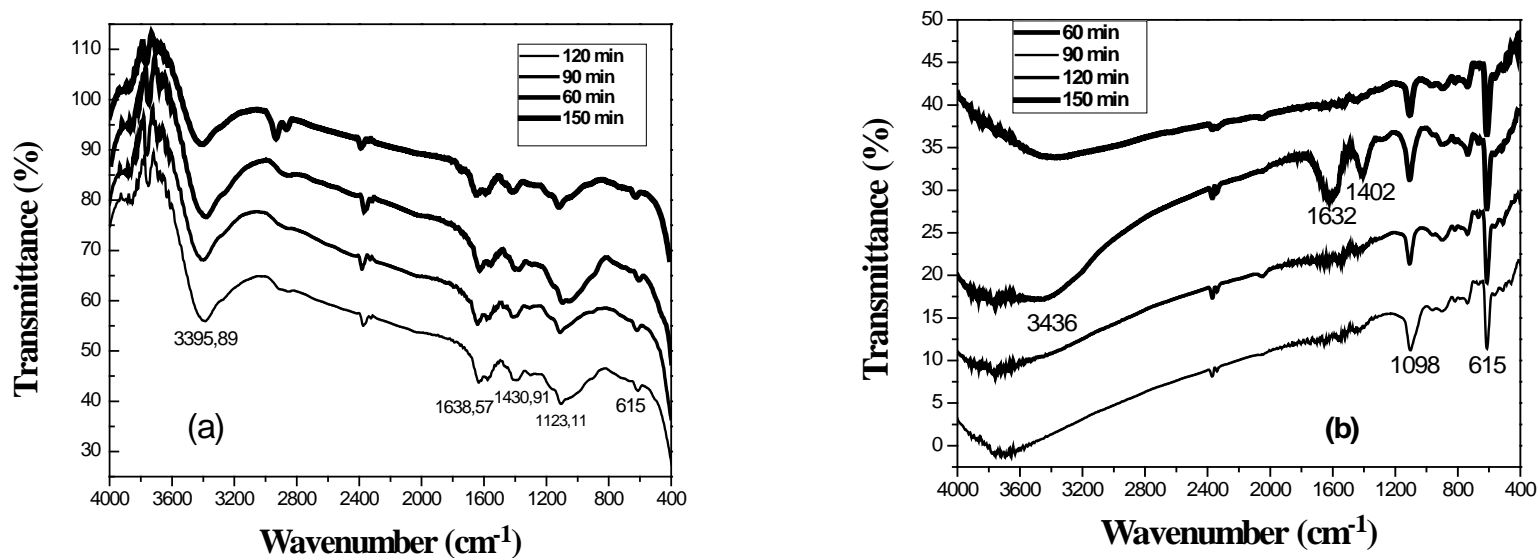


**Fig. 14:** Vertically shifted FTIR spectra of a typical ZnS film deposited at different deposition times, (a) on glass (b) on monocrystalline Si substrate.

## Conclusion

Economical chemical bath deposition (CBD) technique was used to deposit ZnS thin films with high transparency. Thin films of Zinc Sulfide were deposited onto glass substrate from the aqueous solution of Zinc Chloride, ammonia solution, thiourea and tri-sodium citrate ( $C_6H_5Na_3O_7$ ), knowing that  $Na_3$ -citrate was used as non-toxic complexing agent. The influence of the deposition time is investigated in the present work. The thickness of zns films increases nearly lineary with time after the nucleation phase (after 90 min). The X-ray diffraction analysis showed that the as-deposited films are amorphous. An annealing in air improves the film crystallinity with the formation of ZnO phase. The SEM images demonstrate a dense and uniform surface that is free of pits or pinholes. The fine grains are well defined, spherical with different sizes and are uniformly distributed over a smooth and homogeneous surface. The films exhibit also good adherence and cover the entire substrate surface. The EDX analysis confirms the presence of zinc and sulfur in ZnS thin films.

The optical properties of the as-deposited films and annealed at 500°C for 120 minutes are studied. The films are highly transparent. The percentage of transmission is around 82% for all the as-deposited ZnS films in the visible range. While for annealed films case, one measures percentages exceeding 82%, except for the film deposited during 150 min, where the raised limit is 70% when compared with before annealing. The measured band gap was found to be in the range of 3.78 – 4.03 eV depending upon the deposition time.

## References

- [1] Fang XS, Gautam UK, Bando Y, Dierre B, Sekiguchi T, Golberg D. Multiangular branched ZnS nanostructures with needle-shaped tips: Potential luminescent and field emitter nanomaterial; *J Phys Chem C*. 2008; 112:4735-42.
- [2] He JH, Zhang YY, Liu J, Moore D, Bao G, Wang ZL. ZnS/Silica nanocable field effect transistors as biological and chemical nanosensors; *J Phys Chem C*; 2007;111:12152-6.
- [3] Pratap S, Prasad J, Kumar R, Murari K, Singh SS. Preparation & characterisation of IR window grade zinc sulphide powder; *Defence Sci J*. 1996;46:215-21.
- [4] Fang XS, Bando Y, Gautam UK, Zhai TY, Zeng HB, Xu XJ, et al. ZnO and ZnS Nanostructures: Ultraviolet-Light Emitters, Lasers, and Sensors. *Crit Rev Solid State*; 2009; 34:190-223.
- [5] D. Kurbatov, S. Kshnyakina, A. Opanasyuk, V. Melnik, V. Nesprava, Rom. *J. Phys.* 55 (2010) 213
- [6] R. K. Murali, S. Vasantha, K. Rajamma, *Mater. Lett.* 2 (12-13) (2008) 1823
- [7] X. Wu, F. Lai, L. Lin, J. Lv, B. Zhuang, Q. Yan, Z. Huang, *Appl. Surf. Sci.* 254 (2008) 6455-6460
- [8] A. Ateş, M. Ali Yıldırım, M. Kundakçı, A. Astam, *Mater. Sci. Semicond. Process*; 10 (2007) 281.
- [9] P. K. Ghosh, S. Jana, S. Nandy, K. K. Chattopadhyay, *Mater. Res. Bull*; 42 (2007) 505.
- [10] T. Kryshchuk, V.S. Khomchenko, J.A. Andraca-Adame, L.V. Zavyalova, N.N. Roshchina, V.E. Rodionov, V.B. Khachatryan, *Thin Solid Films* 515(2) (2006) 513-516.
- [11] B. A. Bhalerao, D. C. Lokhande, G. B. Wagh, *IEEE. Trans. Nanotechnol.* 12(6), (2013) 996-1001
- [12] D. Balamurugan, B.G. Jeyaprakash, R. Chandiramouli, *J. Appl. Sci.* 12 (2012) 1701-1705.
- [13] N. F. Haubi, K. A. Midhijil, H. G. Rashid, H. L. Mansour, *Mod. Phys. Let. B* 24 (2010)
- [14] F. Gode, C. Gumus, M. Zor, *J. Cryst. Growth* 299 (2007) 136–141.
- [15] Contreras MA, Nakada T, Hongo M, Pudov AO, Sites JR. *Proceedings 3rd World Conference of Photovoltaic Energy Conversion*. 2003; Osaka, Japan:570
- [16] I. O. Oladeji and L. Chow, "Synthesis and processing of CdS/ZnS multilayer films for solar cell application," *Thin Solid Films*, vol. 474, pp. 77-83, 2005.

- [17] F. Göde, C. Umus, and M. Zor, "Investigations on the physical properties of the polycrystalline ZnS thin films deposited by the chemical bath deposition method", *J. Cryst. Growth*, vol. 299, pp. 136-141, 2007.
- [18] Guangxing Liang, Ping Fan, Chaoming Chen, Jingting Luo, Jun Zhao, Dongping Zhang, *J Mater Sci: Mater Electron* (2015) 26:2230–2235.
- [19] Nakada T, Furumi K and Kunioka A 1999 *IEEE Trans. On Elec. Dev.* 46, 2093.
- [20] S. R. Kang, S. W. Shin, D. S. Choi, A. V. Moholkar, J. H. Moon and J. H. Kim, (2010) *Current Applied Physics* 10, S437.
- [21] P. K. Ghosh, M. K. Mitra, K. K. Chattopadhyay, *Nanotechnol.* 16, 107 (2005). [48] C.D. Lokhande, P.S. Patil, H. Tributsch, A. Ennaoui, *Sol. Energy Mat. Sol. Cells* 55 (1998) 379
- [22] C.D. Lokhande, P.S. Patil, H. Tributsch, A. Ennaoui, *Sol. Energy Mat. Sol. Cells* 55 (1998) 379
- [23] S. U. Offiah, P.E. Ugwoke, A.B.C. Ekwealor, S. C. Ezugwu, R.U. Osuji And F. I. Ezema , " Structural And Spectral Analysis Of Chemical Bath Deposited Copper Sulfide Thin Films For Solar Energy Conversions ", *Digest Journal Of Nano Materials And Bio Structures* Vol. 7, No.1, 165 – 173, (2012).
- [24] O. L. Arena, M. T. S. Nair, P. K. Nair, *Semicond. Sci. Technol.*; 12, 1323 (1997).
- [25] H. Yang, J. Zhao, L. Song et al., "Photoluminescent properties of ZnS:Mn nanocrystals prepared in inhomogeneous system"; *Materials Letters*, vol. 57, no. 15, pp. 2287–2291, 2003.